

The cosmological Lithium problem outside the Galaxy: the Sagittarius globular cluster M54 ^{*}

A. Mucciarelli,¹ M. Salaris,² P. Bonifacio³, L. Monaco⁴ and S. Villanova⁵

¹*Dipartimento di Fisica & Astronomia, Università degli Studi di Bologna, Viale Berti Pichat, 6/2 - 40127, Bologna, Italy*

²*Astrophysics Research Institute, Liverpool John Moores University, IC2, 146 Brownlow Hill, Liverpool L3 5RF, United Kingdom*

³*GEPI, Observatoire de Paris, CNRS, Univ. Paris Diderot, 92125, Meudon Cedex, France*

⁴*European Southern Observatory, Casilla 19001, Santiago, Chile*

⁵*Universidad de Concepcion, Casilla 160-C, Concepcion, Chile*

10 November 2021

ABSTRACT

The cosmological Li problem is the observed discrepancy between Li abundance ($A(Li)$) measured in Galactic dwarf, old and metal-poor stars (traditionally assumed to be equal to the initial value $A(Li)_0$), and that predicted by standard Big Bang Nucleosynthesis calculations ($A(Li)_{BBN}$). Here we attack the Li problem by considering an alternative diagnostic, namely the surface Li abundance of red giant branch stars that in a colour magnitude diagram populate the region between the completion of the first dredge-up and the red giant branch bump. We obtained high-resolution spectra with the FLAMES facility at the Very Large Telescope for a sample of red giants in the globular cluster M54, belonging to the Sagittarius dwarf galaxy. We obtain $A(Li) = 0.93 \pm 0.11$ dex, translating – after taking into account the dilution due to the dredge up – to initial abundances ($A(Li)_0$) in the range 2.35–2.29 dex, depending on whether or not atomic diffusion is considered. This is the first measurement of Li in the Sagittarius galaxy and the more distant estimate of $A(Li)_0$ in old stars obtained so far. The $A(Li)_0$ estimated in M54 is lower by ~ 0.35 dex than $A(Li)_{BBN}$, hence incompatible at a level of $\sim 3\sigma$. Our result shows that this discrepancy is a universal problem concerning both the Milky Way and extra-galactic systems. Either modifications of BBN calculations, or a combination of atomic diffusion plus a suitably tuned additional mixing during the main sequence, need to be invoked to solve the discrepancy.

Key words: stars: abundances – stars: atmospheres – stars: Population II – (Galaxy:) globular clusters: individual (M54)

1 INTRODUCTION

Lithium, together with hydrogen and helium, is produced in the first minutes after the Big Bang, and its primordial abundance is a function of the cosmological density of baryons. An estimate of this primordial Li abundance provides therefore an important test for current standard cosmological models. Spite & Spite (1982) first discovered that dwarf (main sequence, turn-off or sub-giants), Population II stars with effective temperatures (T_{eff}) between ~ 5700 and ~ 6300 K and $[Fe/H] < -1.4$ dex share the same Li abundance, the so-called *Spite Plateau*. The existence of a narrow Li *Plateau* has been confirmed by three decades of observations (see e.g. Rebolo et al. 1988; Bonifacio & Molaro 1997;

Asplund et al. 2006; Bonifacio et al. 2007); when considering stellar evolution calculations that include only convection as element transport, this plateau corresponds to the primordial Li abundance in the Galactic halo, that is usually identified as the Li abundance produced during the Big Bang Nucleosynthesis ($A(Li)_{BBN}$). The measured Li abundance in *Spite Plateau* dwarfs is in the range $A(Li) = 2.1$ – 2.3 dex, depending on the adopted T_{eff} scale.

On the other hand, the very accurate determination of the baryonic density obtained from the WMAP (Spergel et al. 2007; Hinshaw et al. 2013) and PLANCK (Planck collaboration 2013) satellites, coupled with the BBN standard model, has allowed to calculate $A(Li)_{BBN}$. The derived values (2.72 ± 0.06 dex, Cyburt et al. 2008, and

^{*} Based on data taken at the ESO, within the observing program 089.D-0341.

¹ $A(Li) = \log \frac{n(Li)}{n(H)} + 12.00$

2.69 ± 0.04 , Coc et al. 2013) are significantly higher, about a factor of 3, than that measured in dwarf stars.

A first potential solution to this discrepancy between $A(Li)_{BBN}$ from BBN calculations and *Spite Plateau* measurements (denoted here as the *cosmological Li problem*) envisages the inclusion of atomic diffusion in stellar model calculations. Atomic diffusion is a physical process that can be modeled parameter-free from first principles, it is efficient in the Sun (see e.g. Bahcall et al. 1997), and can deplete efficiently the surface abundance of Li in metal poor main sequence stars. However, because the degree of depletion increases with effective temperature (and decreasing metallicity), it is not possible to reproduce the observed plateau-like abundance trend (see e.g. Richard et al. 2005, and references therein) if atomic diffusion is fully efficient in objects populating the *Spite Plateau*, see e.g. Fig. 3 in Mucciarelli et al. (2011).

Recent proposed solutions to the *cosmological Li problem* are:

(i) the combined effect of atomic diffusion and some competing additional mixing –necessary to preserve the existence of an abundance *plateau*– whose combined effect decreases the Li abundance in the atmospheres of dwarf stars (Richard et al. 2005; Korn et al. 2006); (ii) inadequacies of the BBN model used to calculate $A(Li)_{BBN}$ (see e.g. Iocco et al. 2009); (iii) a Li depletion driven by Population III stars during the early Galaxy evolution (Piau et al. 2006).

Mucciarelli, Salaris & Bonifacio (2012, MSB12) proposed an alternative/complementary route to investigate the initial Li abundance in Population II stars ($A(Li)_0$), by measuring the surface Li abundance in lower red giant branch (RGB) stars. These stars are located between the completion of the first dredge-up (FDU, where Li-free material is mixed to the surface by convection) and the luminosity level of the RGB bump (where an additional mixing episode occurs, see Gratton et al. 2000). These giants are characterised by a constant Li abundance (at fixed [Fe/H]), drawing a *Plateau* that mirrors the *Spite Plateau* but at a lower abundance ($A(Li) \sim 0.9$ -1.0 dex). The amount of Li depletion due to dilution after the FDU can be predicted easily by stellar models. Lower RGB stars are therefore a powerful alternative diagnostic of $A(Li)_0$, mainly because the derived value is very weakly affected by atomic diffusion during the previous main sequence phase. This means that it is possible to put strong constraints on $A(Li)_0$, irrespective of whether atomic diffusion is effective or not, and assess whether additional processes –within the stars, or during the BBN nucleosynthesis, or during Galaxy formation– need to be invoked to match the BBN calculations of Li abundances. Moreover, lower RGB stars also enable to investigate $A(Li)_0$ in stars more distant than those usually observed for *Spite Plateau* studies.

In this paper we exploit this new diagnostic with the aim to study $A(Li)_0$ in M54, a massive globular cluster (GC) immersed in the nucleus of the Sagittarius (Sgr) dwarf galaxy (Monaco et al. 2005; Bellazzini et al. 2008). The dwarf stars in M54 and Sgr are too faint ($V \sim 22$) to be observed, thus the study of lower RGB stars represents the only possible route to infer $A(Li)_0$ in this galaxy. Section 2 describes the spectroscopic observations, followed in Section 3 by the determination of the Li abundances and

the constraints on $A(Li)_0$ for M54 stars, and is followed by a discussion of the results and conclusions.

2 OBSERVATIONS

High-resolution spectra of lower RGB stars in M54 have been secured with the multi-object spectrograph FLAMES (Pasquini et al. 2002) at the ESO Very Large Telescope, in the GIRAFFE/MEDUSA mode. The observations have been performed with the setups HR12 (to sample the Na D lines, with a resolution of 18700) and HR15N (to sample the Li doublet at 6707 Å, with a resolution of 17000). The same target configuration has been used for both gratings and each target has been observed for a total time of 26 hr and 4 hr, for HR15N and HR12, respectively.

The targets have been selected from ACS@HST photometry (Siegel et al. 2007) for the central region and from WFI@ESO photometry (Monaco et al. 2002) for the outermost region. Eighty-five stars have been selected along the RGB of M54 in the magnitude range $V=18.3$ -18.6, being its RGB bump at $V \sim 18$, according to the RGB luminosity function. We excluded the 0.2 magnitudes below the RGB bump to minimise the contamination from the Sgr He-Clump stars. Figure 1 shows the colour-magnitude diagram of M54 with marked the observed targets (red and blue points). The signal-to-noise (SNR) ratio per pixel around the Li doublet ranges from ~ 30 to ~ 50 , with an average value of 42.

The spectra have been processed with the GIRAFFE data reduction pipeline, including bias-subtraction, flat-fielding, wavelength calibration, spectral extraction². Radial velocities have been measured with DAOSPEC (Stetson & Pancino 2008) by using ~ 15 metallic lines. 11 targets have been discarded because they are clearly Galactic interlopers, with radial velocities between -105 and $+60$ km/s (see Fig. 8 in Bellazzini et al. 2008). Finally, our sample includes a total of 74 candidate member stars of M54 (their main information is listed in Table 1).

3 CHEMICAL ANALYSIS

Values of T_{eff} have been derived from the $(V-I)_0$ colour by means of the calibration by Alonso et al. (1999), adopting the colour excess $E(B-V) = 0.14$ mag (Layden & Sarajedini 2000) and the extinction coefficients by McCall (2004). Surface gravities have been calculated from the Stefan-Boltzmann relation assuming the photometric T_{eff} , the bolometric corrections by Alonso et al. (1999) and the distance modulus $(m-M)_0 = 17.10$ mag (Monaco et al. 2004). We assumed a mass of $0.8 M_\odot$, according to a BaSTI isochrone (Pietrinferni et al. 2006) with 12 Gyr, $Z = 0.0003$ and α -enhanced chemical mixture. A microturbulent velocity $v_{turb} = 1.5$ km/s has been assumed for all the targets, taking the median value of v_{turb} of the lower RGB stars analysed by MSB12.

Fe and Na abundances have been derived from the line equivalent widths (EWs) by using the code GALA

² <https://www.eso.org/sci/software/pipelines/>

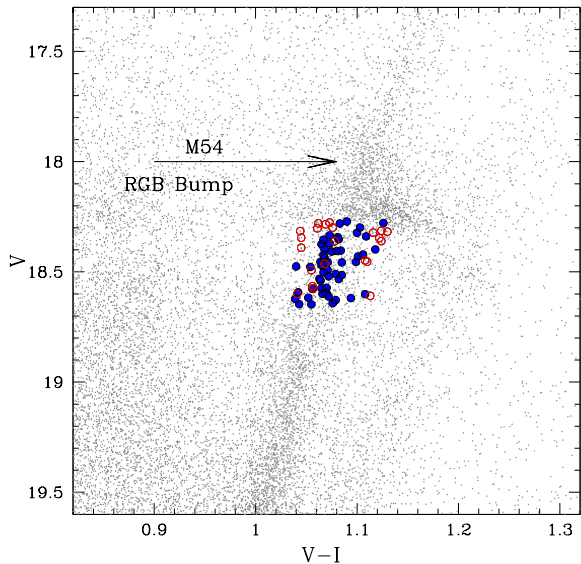


Figure 1. Colour-magnitude diagram of M54+Sgr that displays also the observed targets. Blue filled circles denote the member stars of M54, red empty circles the Sgr field stars.

(Mucciarelli et al. 2013), coupled with ATLAS9 model atmospheres. Fe abundances have been obtained from the measure of ~ 10 -15 Fe I lines, while Na abundances from the Na D lines at 5889-5895 Å. EWs of Fe lines have been measured with DAOSPEC (Stetson & Pancino 2008), while those of the Na lines by using IRAF assuming a Voigt profile. NLTE corrections for the Na abundances are from Gratton et al. (1999). The recent NLTE calculations by Lind et al. (2011) provide $[Na/Fe]_{NLTE}$ lower by about 0.2–0.3 dex; however, in the following we refer to the abundances obtained with the corrections by Gratton et al. (1999) to allow a direct comparison with Carretta et al. (2010) that measured Na abundances in 76 stars of M54. Figure 2 shows the metallicity distribution of the 74 candidate M54 member stars, ranging from $[Fe/H] = -2.0$ dex up to -0.34 dex, with a main peak at ~ -1.7 dex and a second peak at ~ -0.9 dex.

We consider as members of M54: (i) stars with radial velocity between 100 and 170 km/s, (Bellazzini et al. 2008), and (ii) stars with $[Fe/H] < -1.3$ dex, in order to exclude the stars of the second peak observed in the metallicity distribution, likely belonging to the Sgr field (note that the metallicity distributions of M54 by Bellazzini et al. 2008 and Carretta et al. 2010 are both broad but they do not show evidence of bimodality). Finally, 51 targets are considered as *bona fide* M54 member stars. These stars are shown as blue circles in Fig. 1 and as the shaded histogram in Fig. 2. The mean iron content is $[Fe/H] = -1.67 \pm 0.02$ dex ($\sigma = 0.15$ dex), compatible with those derived by Bellazzini et al. (2008) and Carretta et al. (2010). The M54 member stars show a wide range of $[Na/Fe]$, between -0.56 and $+0.77$ dex, with an average value $[Na/Fe] = +0.11 \pm 0.04$ dex ($\sigma = 0.31$ dex), fully consistent with the results by Carretta et al. (2010).

The Li abundances have been derived from the Li resonance doublet at ~ 6707 Å, by comparing the observed spectra with a grid of synthetic spectra, calculated with the

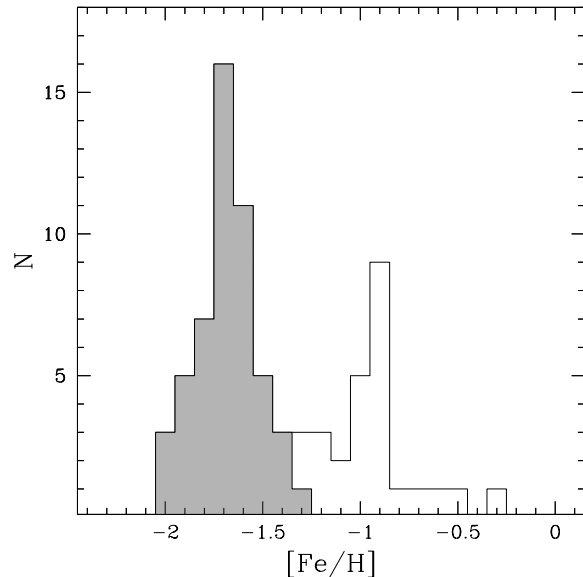


Figure 2. $[Fe/H]$ distribution for the RGB stars of M54. The grey shaded histogram includes the targets considered as members of M54, according to radial velocity and iron content.

code SYNTHE (Sbordone et al. 2004). NLTE corrections are from Lind et al. (2008). The uncertainty in the fitting procedure has been estimated with MonteCarlo simulations performed by analysing synthetic spectra with the injection of Poissonian noise. Also, we included in the total error budget of the Li abundance the impact of the uncertainties in T_{eff} , the other parameters having a negligible impact on $A(Li)$. Because of the weakness of the Li doublet ($EW \sim 13$ mÅ), at the SNR of our spectra it cannot be properly measured in each individual spectrum. Thus, we grouped together all the spectra of the stars considered as members of M54, obtaining an average spectrum with $SNR \sim 300$ and assuming the average atmospheric parameters of the sample, namely $T_{eff} = 4995$ K and $\log g = 2.46$. These stars are located in a narrow region of the colour-magnitude diagram, legitimating this procedure. In particular, T_{eff} is the most critical parameter for the Li abundance estimate, whereas $\log g$ and v_{turb} have a negligible impact. The 51 cluster members cover a T_{eff} range between 4873 K and 5090 K, with a mean equal to 4995 K ($\sigma = 48$ K), and a median value of 5005 K with an interquartile range of 51 K. Figure 3 shows the Li doublet observed in the average spectrum, with superimposed the best-fit synthetic spectrum (red solid line) and two synthetic spectra calculated with ± 0.2 dex with respect to the best-fit abundance (red dashed lines).

The final derived Li abundance is $A(Li)_{NLTE} = 0.93 \pm 0.03 \pm 0.11$ dex (where the first errorbar is the internal error as derived by the MonteCarlo simulations, and the second one is due to the T_{eff} uncertainty). For consistency with MSB12 we checked also $A(Li)_{NLTE}$ obtained with the NLTE corrections by Carlsson et al. (1994), that lead to an increase of the final abundance by 0.08 dex, thus providing $A(Li)_{NLTE} = 1.01$ dex. The choice of the NLTE corrections has obviously a small impact of the final $A(Li)$ value and does not change drastically our conclusions.

3.1 Checks about the average spectrum

To assess the stability of our results against the way we group the spectra, we have performed a number of sanity checks. In these tests we divided the cluster sample into two bins, according to:

- (a) $[\text{Fe}/\text{H}]$; the two groups include stars with $[\text{Fe}/\text{H}]$ lower and higher than the median value of $[\text{Fe}/\text{H}]$ ($[\text{Fe}/\text{H}] = -1.67$; see Fig. 2) respectively;
- (b) T_{eff} ; the boundary between the two groups is the median T_{eff} ;
- (c) magnitude; the two groups include stars fainter and brighter than the median V-band magnitude ($V = 18.45$) respectively;
- (d) $[\text{Na}/\text{Fe}]$; the boundary between the two groups is the median value of the $[\text{Na}/\text{Fe}]_{\text{NLTE}}$ distribution ($[\text{Na}/\text{Fe}]_{\text{NLTE}} = +0.16$ dex).

For all these cases, we found $A(\text{Li})_{\text{NLTE}}$ compatible within the uncertainties with the value obtained with the average spectrum of the whole cluster targets, as shown by Fig. 4. The largest difference (0.08 dex, still compatible within 1σ with the original value), is found when we group together spectra with V-band magnitude fainter than $V = 18.45$, because they have the lowest SNR. In light of these results, we can conclude that no significant biases related to the grouping of the target spectra affect our Li abundance estimate.

Another point to discuss here concerns the use of a single value of the NLTE correction computed for the average atmospheric parameters of the whole sample. To this purpose we notice that the variation of the NLTE corrections in the parameter space covered by our targets is small: in particular, at fixed $T_{\text{eff}}/\log g$ the corrections vary by ~ 0.03 – 0.04 dex between the minimum and maximum $[\text{Fe}/\text{H}]$ of the metallicity distribution, while at fixed metallicity, the corrections change by ~ 0.03 dex between the minimum and maximum T_{eff} . To investigate more rigorously this effect, we simulated a spectrum with the following procedure: (1) for each individual member star a synthetic spectrum has been calculated with the appropriate atmospheric parameters and iron abundance, imposing a Li abundance $A(\text{Li})_{\text{NLTE}} = 0.93$ dex (to take into account the proper NLTE correction of each star); (2) the spectra have been rescaled according to the relative differences in magnitude; (3) Poissonian noise has been injected in each synthetic spectrum to reproduce the measured SNR of the observed counterpart; (4) all these synthetic spectra have been co-added as done with the observed sample.

The entire procedure is repeated to obtain a sample of 1000 average spectra that has been analysed as done with the observed stars. The derived $A(\text{Li})_{\text{NLTE}}$ distribution (assuming a single value of the NLTE correction) displays a mean value equal to 0.95 dex with a dispersion of 0.04 dex. This simulation confirms that star-to-star variations of the NLTE corrections are only a second order effect and do not affect substantially the abundance derived from the average spectrum.

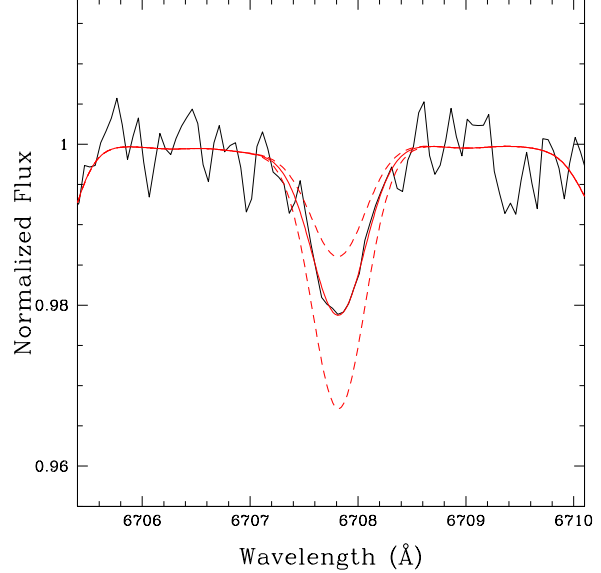


Figure 3. The observed Li doublet of the average spectrum obtained by combining all 51 targets that are members of M54. The red solid line is the best-fit synthetic spectrum, whilst the red dashed lines display the synthetic spectra calculated with ± 0.2 dex variations with respect to the best-fit abundance.

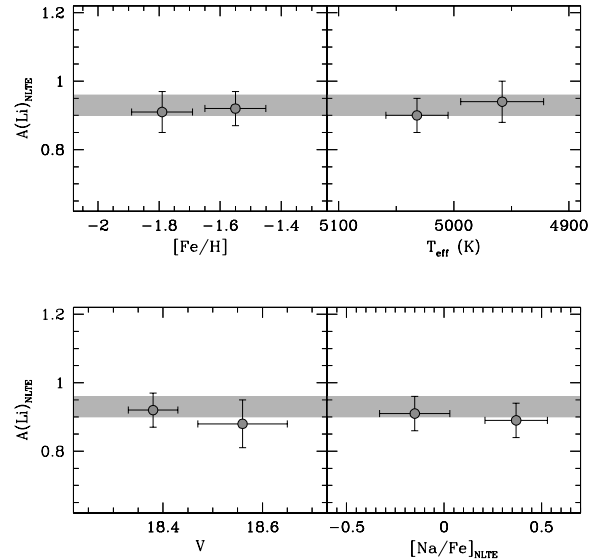


Figure 4. $A(\text{Li})_{\text{NLTE}}$ values (dark grey circles) obtained by grouping the sample of M54 member stars into two average spectra according to the median value of $[\text{Fe}/\text{H}]$ (left upper panel), T_{eff} (right upper panel), V-band magnitude (left lower panel) and $[\text{Na}/\text{Fe}]_{\text{NLTE}}$ (right lower panel). Abundance errorbars include only the internal uncertainty from MonteCarlo simulations. Errorbars along the x-axis denote the 1σ spread around the mean value of each quantity. The shaded grey area in each panel denotes the $\pm 1\sigma$ range with respect to the $A(\text{Li})_{\text{NLTE}}$ obtained from the average spectrum of the whole M54 sample.

3.2 Lithium abundance and chemical anomalies in GCs

It is well established that individual GCs harbour sub-populations characterised by different abundances of light elements, like Na and O (see e.g. Gratton et al. 2012). In principle, these so-called *second-generation* stars, characterised by high values of [Na/Fe] and low values of [O/Fe], should display lower Li abundances, because they are predicted to be born from gas diluted with Li-poor material coming from asymptotic giant branch or fast-rotating massive stars. Given that the thermonuclear reactions able to produce the observed chemical patterns occur at temperatures larger than $\sim 10^7$ K, while Li is destroyed at lower temperatures ($\sim 2.5 \cdot 10^6$ K), second-generation stars should exhibit lower abundances of Li compared to first-generation stars. In particular, Li depletions, Li-O correlations and Li-Na anticorrelations are expected within individual clusters. Empirically, clear Li-O correlations have been detected in NGC6752 (Shen et al. 2010) and 47 Tuc (Dobrovolskas et al. 2014). Three Na-rich stars (thus belonging to the second cluster generation) with low Li abundance ($A(\text{Li}) < 2.0$ dex) have been detected in NGC6397 (Lind et al. 2009), while most of the observed stars display a uniform Li (compatible with the *Spite Plateau*) but a large range of Na, suggesting that Li depletion is negligible for the second generation stars of this cluster. M4 displays a very small (if any) intrinsic Li dispersion, without correlation between O and Li abundance (Mucciarelli et al. 2011) and with a weak Li-Na anticorrelation (Monaco et al. 2012). Lower RGB stars in M12 share all the same Li content, whilst there is a spread of Li in M5, but no statistically significant Li-O correlations and Li-Na anticorrelations (D’Orazi et al. 2014).

We have checked whether potential systematic differences between $A(\text{Li})$ of first and second generation stars in M54 can affect our conclusions. As discussed in Section 3.1 we divided the sample of M54 stars into two groups, according to their [Na/Fe] abundances, adopting as boundary the median value of the [Na/Fe] distribution (+0.16 dex). The derived average spectra show a very similar Li content, $A(\text{Li})_{NLTE} = 0.91 \pm 0.05$ and 0.89 ± 0.05 dex for the Na-poor and Na-rich groups, respectively, consistent with the value for the whole sample (see left bottom panel in Fig. 4). Note that systematic differences in the Li content between the two samples smaller than ~ 0.1 dex (compatible, for instance, with those observed by Monaco et al. 2012 in M4) cannot be ruled out. However, such a small possible Li depletion in Na-rich stars of M54 does not change our conclusion about $A(\text{Li})_0$ in this cluster.

3.3 $A(\text{Li})_0$ in M54

To constrain the initial $A(\text{Li})_0$ in M54, we adopted the same procedure discussed in MSB12, by using the amount of Li depletion due to the FDU as predicted by stellar models (see their Table 2). For a metallicity $[\text{Fe}/\text{H}] = -1.67$ dex, the predicted value is equal to 1.36 dex and 1.42 dex without and with atomic diffusion, respectively. As already discussed by MSB12, the amount of Li depletion along the RGB Plateau is marginally sensitive to the efficiency of the atomic diffusion that affects the dwarf stars much more strongly. We recall that M54 has an intrinsic iron dispersion (Carretta et al.

2010); however, the predicted Li depletion changes by ± 0.02 dex with respect to the values quoted above if we consider the minimum and maximum value of the cluster metallicity distribution, namely $[\text{Fe}/\text{H}] = -2.0$ and -1.3 dex. We can thus neglect the effect of the cluster metallicity spread.

The derived $A(\text{Li})_0$ in M54 is $A(\text{Li})_0 = 2.29 \pm 0.11$ dex (the error bar takes into account only the dominant effect of the uncertainty in T_{eff}) without diffusion and 2.35 ± 0.11 dex with fully efficient diffusion. When the NLTE corrections by Carlsson et al. (1994) are adopted, the range of $A(\text{Li})_0$ values is 2.37–2.43 dex.

4 DISCUSSION

This is the first study of the primordial Li abundance in M54 and, hence, in the Sgr galaxy. Also, it is the most distant measurement of $A(\text{Li})$ in old, metal-poor stars obtained so far, given that Li abundance determinations in dwarf stars are restricted to distances within ~ 8 kpc from the Sun (see the case of M92, Boesgaard et al. 1998; Bonifacio 2002). The use of lower RGB stars allows a giant leap in the study of $A(\text{Li})_0$, pushing our investigation to ~ 25 kpc from the Sun and enlarging our perspective of the Li problem. This work demonstrates the potential of lower RGB stars to investigate $A(\text{Li})_0$ in stellar systems for which the observation of dwarf stars is precluded.

Fig. 5 compares our $A(\text{Li})$ and $A(\text{Li})_0$ for M54 stars (red empty and filled circle, respectively) to the results of Galactic field dwarf (grey circles) and lower RGB stars (grey squares). The value of $A(\text{Li})_{BBN}$ provided by Coc et al. (2013) is shown as reference. First of all, $A(\text{Li})$ measured in M54 red giants is in very good agreement with the results for the Galactic halo field (MSB12 found an average $A(\text{Li}) = 0.97$ with the same T_{eff} scale used for this study). Secondly, $A(\text{Li})_0$ inferred from the lower RGB of M54 has, as already said, a very small dependence on whether atomic diffusion is fully efficient or inhibited, and results to be on average $\sim 0.04 - 0.10$ dex higher than typical $A(\text{Li})$ values measured in dwarf stars, that are equal on average to $A(\text{Li}) \sim 2.25$ dex (see Fig. 5). Assuming the initial Li in M54 and the Galactic halo was the same, if atomic diffusion is fully efficient in *Spite Plateau* stars within the range of metallicities covered by M54 lower RGB stars, their surface Li abundances should be 0.4–0.7 dex lower than $A(\text{Li})_0$ (see e.g. Fig. 3 in Mucciarelli et al. 2011)³.

This means that either atomic diffusion is completely inhibited in halo field stars, and therefore the cosmological Li problem persists, or an additional element transport must be at work, burning during the main sequence more Li than predicted by models with diffusion only. This route has been investigated in order to interpret the surface Li abundances measured in dwarf stars of Galactic globular clusters.

To this purpose we first compare the results for M54 with measurements of $A(\text{Li})$ obtained for lower RGB stars in Galactic GCs that do not display a significant spread of Li.

³ It is worth bearing in mind that a detailed comparison between $A(\text{Li})_0$ derived from lower RGB stars and the *Spite Plateau* depends also on the adopted T_{eff} scales and NLTE corrections; here we simply take at face value the various estimates displayed in Fig. 5

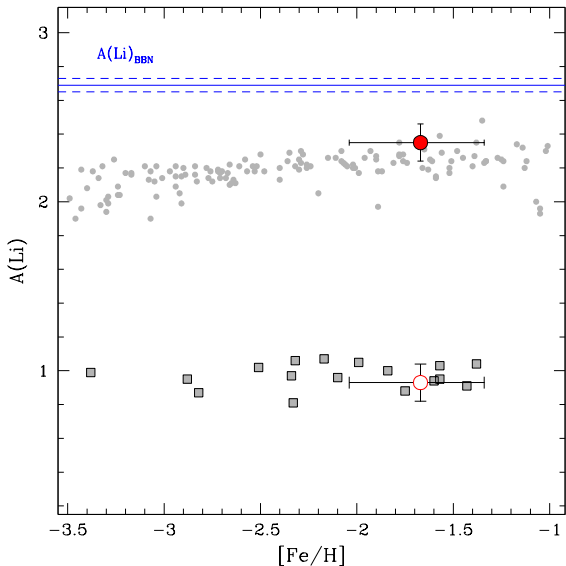


Figure 5. Li abundance as a function of $[\text{Fe}/\text{H}]$ for *Spite Plateau* and lower RGB field halo stars. Grey circles denote the dwarf sample (Bonifacio & Molaro 1997; Asplund et al. 2006; Aoki et al. 2009; Hosford et al. 2009; Melendez et al. 2010), and grey squares the lower RGB stars by MSB12. The empty red circle denotes the surface $A(\text{Li})$ in the lower RGB stars of M54, while the filled red circle displays the derived $A(\text{Li})_0$ assuming fully efficient atomic diffusion (the horizontal errorbars associated to M54 data represent the range of $[\text{Fe}/\text{H}]$ covered by the cluster). The blue solid line denotes $A(\text{Li})_{\text{BBN}}$ (Coc et al. 2013), with the $\pm 1\sigma$ uncertainty denoted by blue dashed lines.

MSB12 determined $A(\text{Li})=1.00$ and $A(\text{Li})=0.92$ dex (both with ~ 0.10 dex error bars) for NGC6397 ($[\text{Fe}/\text{H}] \sim -2.1$ dex) and M4 ($[\text{Fe}/\text{H}] \sim -1.1$ dex) respectively, using the same T_{eff} scale employed here. The same result has been found for lower RGB stars in M4 by Villanova & Geisler (2011). These values are well consistent with M54 result. The recent study by D’Orazi et al. (2014) found again a similar value, $A(\text{Li})=0.98$ dex, with an error bar of ~ 0.10 dex (using again the same T_{eff} scale of this work) for lower RGB stars in M12, another cluster with essentially no Li spread amongst lower RGB objects, and $[\text{Fe}/\text{H}]$ similar to M54.

Measurements of $A(\text{Li})$ in dwarf stars have been performed in M92 (Boesgaard et al. 1998; Bonifacio 2002) NGC6397 (Korn et al. 2006; Lind et al. 2008; Gonzalez Hernandez et al. 2009; Nordlander et al. 2012), NGC6752 (Shen et al. 2010; Gruyters et al. 2013, 2014), M4 (Mucciarelli et al. 2011; Monaco et al. 2012), 47 Tuc (D’Orazi et al. 2010; Dobrovolskas et al. 2014). To these GCs, we add also Omega Centauri (Monaco et al. 2010), a globular cluster-like stellar system characterized by a wide range of metallicities and probably ages, and usually thought as the stripped core of a dwarf galaxy. All these works found that dwarf GC stars display on average a Li content compatible with the *Spite plateau*, confirming cosmological Li problem. The works on NGC6397 and NGC6752 by Gruyters et al. (2013) and Gruyters et al. (2014) have however addressed this issue by considering as potential solution the combined effect of atomic diffusion and an hypothetical extra mixing process. In the following we will consider the

recent analysis by Gruyters et al. (2014) of Li abundances in NGC6752, that has a $[\text{Fe}/\text{H}]$ very close to the mean value of M54. These authors followed the same procedures applied to infer $A(\text{Li})_0$ in NGC6397 (see Nordlander et al. 2012, for the latest work on this cluster). They measured the abundances of Li, and additional metals like Mg, Ca, Ti and Fe, in cluster stars from the main sequence turn off to the lower red giant branch, and compared the abundance trends along these evolutionary phases with results from stellar model calculations by Richard et al. (2002). The observed trends could be matched only by models where the effect of diffusion was modulated by an additional mixing that in Richard et al. (2002) calculations is modeled as a diffusive process with diffusion coefficient D_T chosen as

$$D_T = 400D_{\text{He}}(T_0) \left[\frac{\rho}{\rho(T_0)} \right]^{-3} \quad (1)$$

where $D_{\text{He}}(T_0)$ is the atomic diffusion coefficient of He at a reference temperature T_0 , and $\rho(T_0)$ is the density of the stellar model at the same temperature. This is a somewhat ad-hoc prescription, with the proportionality constant $400D_{\text{He}}(T_0)$, and the steep dependence on ρ being essentially free parameters. A justification for the choice of the steep dependence on ρ stems from the need to restrict the efficiency of this mixing to a narrow region below the outer convection zone, as suggested by the solar beryllium abundance, believed to be essentially unaltered since the formation of the solar system. The temperature T_0 is also a free parameter, that determines the depth where this diffusive mixing is most effective. It is important to remark that so far there has not been any attempt to test whether this mixing prescription can be associated to a well established physical process like, i.e., rotationally induced mixing. Assuming that the prescription in Eq. 1 is realistic, Gruyters et al. (2014) found that the free parameter T_0 has to be set to $\log(T_0)=6.2$ to match the observed abundance trends for NGC6752, resulting in $A(\text{Li})_0=2.53 \pm 0.10$, within less than 2σ of the BBN predictions.

To our purposes it is relevant to notice that when $\log(T_0)=6.2$, the lower RGB abundances of Richard et al. (2005) models decrease by ~ 0.1 dex compared to the case of pure diffusion, because during the main sequence additional Li is transported to the burning region by this extra mixing. If the same process and the same efficiency estimated for NGC6752 are assumed also for M54, we need to add the same amount to $A(\text{Li})_0$ determined including efficient diffusion, thus obtaining $A(\text{Li})_0 \sim 2.45 \pm 0.11$ dex (or $A(\text{Li})_0 \sim 2.53 \pm 0.11$ dex when considering the NLTE corrections by Carlsson et al. 1994).

Given the current lack of identification of the proposed additional mixing with an established physical process, it is fair to say that we should be still cautious about this route to solve the cosmological Li problem, because simple parametric models have little predictive power. For example, to explain abundance trends in NGC6397, NGC6752 and M4 –and reconcile the measured $A(\text{Li})$ with $A(\text{Li})_{\text{BBN}}$ – one needs to employ a varying value of T_0 , generally increasing with increasing $[\text{Fe}/\text{H}]$. Whether or not this trend of T_0 with $[\text{Fe}/\text{H}]$ is a sign of the inadequacy of this parametrization of the additional mixing, requires a deeper understanding of its origin.

Observationally, Gonzalez Hernandez et al. (2009)

found a trend of the surface $A(\text{Li})$ with T_{eff} in NGC6397 that is not explainable with the additional mixing of Eq. 1. Also, as discussed by Dobrovolskas et al. (2014), the constant Li abundance observed among the stars in Omega Centauri (Monaco et al. 2010) spanning a wide range of ages and metallicities, and the Li distribution observed in 47 Tuc seem to require fine-tuned mechanisms that are at present difficult to explain with simple parametric diffusive mixing prescriptions.

5 CONCLUSIONS

We measured the surface Li abundance in lower RGB stars harboured by M54, a GC belonging to the Sgr dwarf galaxy. We have obtained $A(\text{Li}) = 0.93 \pm 0.11$ dex, in agreement with measurements in Galactic halo stars. By considering the dilution due to the FDU, we have established an initial Li abundance of this stellar system ($A(\text{Li})_0 = 2.29 \pm 0.11$ and 2.35 ± 0.11 dex, without and with atomic diffusion, respectively) that is lower than the BBN value by ~ 0.3 dex. The cluster $A(\text{Li})_0$ can become compatible with $A(\text{Li})_{\text{BBN}}$ within $\sim 2\sigma$ only assuming diffusion plus the additional mixing prescriptions by Richard et al. (2005) calibrated on the (same metallicity) Galactic GC NGC6752 (Gruyters et al. 2014). Alternatively, inadequacies of the BBN model used to derive $A(\text{Li})_{\text{BBN}}$ cannot be totally ruled out.

Also, an important question can be addressed by our study: is the Li problem a *local* problem, limited to our Galaxy, or is it independent of the environment? The analysis of the RGB stars in M54 confirms the findings in ω Centauri (Monaco et al. 2010), considered as the remnant of an accreted dwarf galaxy: *the Li problem seems to be an universal problem, regardless of the parent galaxy*. The solution able to explain the discrepancy must work both in the Milky Way and other galaxies, with different origins and star formation histories. Thus, it seems unlikely that the scenario proposed by Piau et al. (2006), requiring that at least one third of the Galactic halo has been processed by Population III, massive stars, can work in the same way also in smaller systems like Sgr and ω Centauri (see also Prantzos 2007). The universality of the *Spite plateau* and the lower RGB abundances is a constraint that must be satisfied by any theory aimed at solving the cosmological Li problem.

We warmly thank the referee, Andreas Korn, for his detailed comments that have helped to improve the paper significantly. S.V. gratefully acknowledges the support provided by Fondecyt reg. N. 1130721.

REFERENCES

- Alonso, A. Arribas, S. & Martinez-Roger, C., 1999, A&AS, 140, 261
Aoki, W., et al., 2009, ApJ, 698, 1803
Asplund, M., Lambert, D. L., Nissen, P. E., Primas, F., & Smith, V. V., 2006, ApJ, 644, 229
Bahcall, J. N.; Pinsonneault, M. H., Basu, S., & Christensen-Dalsgaard, J., 1997, PhRvL, 78, 171
Bellazzini, M., et al., 2008, AJ, 136, 1147
Boesgaard, A. M., Deliyannis, C. P., Stephens, A., & King, J. R., 1998, 493, 206
Bonifacio, P. & Molaro, P., 1997, MNRAS, 285, 847
Bonifacio, P., 2002, A&A, 395, 515
Bonifacio, P., et al. 2007, A&A, 462, 851
Carlsson, M., Rutten, R. J., Bruls, J. H. M. J., & Shchukina, N. G., 1994, A&A, 288, 860
Carretta, E., et al., 2010, A&A, 520, 95
Coc, A., Uzan, J.-P., & Vangioni, E., 2013, arXiv1307.6955
Cyburt, R. H., Fields, B. D., & Olive, K. A., 2008, J. Cosmol. Astro-Part. Phys., 11, 12
Dobrovolskas, V, Kucinkas, A., Bonifacio, P., Korotin, S. A., Steffen, M., Sbordone, L., Caffau, E., Ludwig, H.-G., Royer, F., & Prakapavicius, D., 2014, A&A, 565, 121
D’Orazi, V., Lucatello, S., Gratton, R., Bragaglia, A., Carretta, E., Shen, Z., & Zaggia, S., 2010, ApJ, 713L, 1
D’Orazi, V., Angelou, G. C., Gratton, R. G., Lattanzio, J. C., Bragaglia, A., Carretta, E., Lucatello, S., & Momany, Y., 2014, ApJ, in press (arXiv:1406.5513)
Gonzalez Hernandez, J. I., Bonifacio, P., Caffau, E., Steffen, M., Ludwig, H.-G., Behara, N. T., Sbordone, L., Cayrel, R., & Zaggia, S., 2009, A&A, 505L, 13
Gratton, R. G., Carretta, E., Eriksson, K., & Gustafsson, B., 1999, A&A, 350, 955
Gratton, R. G., Sneden, C., Carretta, E., & Bragaglia, A., 2000, A&A, 354, 169
Gratton, R. G., Carretta, E., & Bragaglia, A., 2012, A&ARv, 20, 50
Gruyters, P., Korn, A. J., Richard, O., Grundahl, F., Collet, R., Mashonkina, L. I., Osorio, Y., & Barklem, P. S., 2013, A&A, 555, 31
Gruyters, P., Nordlander, T., & Korn, A. J., 2014, arXiv1405-6543
Hinshaw, G., et al., 2013, ApJS, 208, 19
Hosford, A., Ryan, S. G., Garcia Perez, A. E., Norris, J. E., & Olive, K. A., 2009, A&A, 493, 601
Korn, A. J., et al., 2006, Nature, 442, 657
Iocco, F., Mangano, G., Miele G., Pisanti, O., & Serpico, P. D., 2009, PhR, 472, 1
Layden, A. C., & Sarajedini, A., 2000, AJ, 119, 1760
Lind, K., Asplund, M., Barklem, P. S., & Belyaev, A. K., 2008, A&A, 528, 103
Lind, K., Primas, F., Charbonnel, C., Grundahl, F., & Asplund, M., 2009, 503, 545
Lind, K., Asplund, M., Barklem, P. S., & Belyaev, A. K., 2011, A&A, 528, 103
McCall, M. L., 2004, AJ, 128, 2144
Melendez, J., Casagrande, L., Ramirez, I., Asplund, M. & Schuster, W. J., 2010, A&A, 515, L3
Monaco, L., Ferraro, F. R., Bellazzini, M., & Pancino, E., 2002, ApJ, 578L, 47
Monaco, L., Bellazzini, M., Ferraro, F. R., & Pancino, E., 2004, MNRAS, 353, 874
Monaco, L., Bellazzini, M., Ferraro, F. R., & Pancino, E., 2005, MNRAS, 356, 1396
Monaco, L., Bonifacio, P., Sbordone, L., Villanova, S., & Pancino, E., 2010, A&A, 519L, 3
Monaco, L., Villanova, S., Bonifacio, P., Caffau, E., Geisler, D., Marconi, G., Momany, Y., & Ludwig, H.-G., 2012, A&A, 539, 157
Mucciarelli, A., Salaris, M., Lovisi, L., Ferraro, F. R., Lanzoni, B., Lucatello, S., & Gratton, R. G., 2011, MNRAS,

- 412, 81
Mucciarelli, A., Salaris, M. & Bonifacio, P., 2012, MNRAS, 419, 2195
Mucciarelli, A., Pancino, E., Lovisi, L., Ferraro, F. R., & Lapenna, E., 2013, ApJ, 766, 78
Nordlander, T., Korn, A. J., Richard, O., & Lind, K., 2012, ApJ, 753, 48
Pasquini, L., 2002, The Messenger, 110, 1
Piau, L. et al., 2006, ApJ, 653, 300
Pietrinferni, A., Cassisi, S., Salaris, M., & Castelli, F., 2006, ApJ, 642, 797
Planck Collaboration, 2013, arXiv1203.5076
Prantzos, N., 2007, SSRv, 130, 27
Rebolo, R., Beckman, J. E., & Molaro, P., 1988, A&A, 192, 192
Richard, O., Michaud, G., & Richer, J., 2002, ApJ, 580, 1100
Richard, O., Michaud, G., & Richer, J., 2005, ApJ, 619, 538
Sbordone, L., Bonifacio, P., Castelli, F., & Kurucz, R. L., 2004, MSAIS, 5, 93
Shen, Z.-X., Bonifacio, P., Pasquini, L., & Zaggia, S., 2010, A&A, 524L, 2
Siegel, M. H., et al., 2007, ApJ, 667L, 57
Spergel, D. N., et al., 2007, ApJS, 170, 377
Spite, M., & Spite, F., 1982, Nature, 297, 483
Stetson, P. & Pancino, E., 2008, PASP, 120, 1332
Villanova, S. & Geisler, D., 2011, A&A, 535, 31

Table 1. Identification numbers, coordinates, effective temperature, surface gravity, radial velocity, [Fe/H] and [Na/Fe] abundances. Final flag indicates the membership to M54 or to Sgr.

ID	RA (J2000)	Dec (J2000)	T_{eff} (K)	log g	RV (km/s)	[Fe/H] (dex)	[Na/Fe] (dex)	flag
6750	283.7948303	-30.4990501	5010	2.50	130.5	-1.75	-0.56	M54
7590	283.7933655	-30.4935970	5010	2.51	140.9	-1.65	0.38	M54
12291	283.7864380	-30.5019646	4987	2.47	151.8	-2.00	-0.40	M54
21190	283.7769165	-30.5052319	4921	2.40	135.7	-1.74	0.16	M54
51661	283.7530823	-30.5037270	4916	2.41	148.5	-0.34	-0.48	Sgr
53985	283.7514343	-30.4937611	4936	2.37	149.1	-1.74	0.09	M54
56686	283.7486572	-30.5045719	5018	2.45	141.6	-1.42	0.25	M54
65022	283.7391968	-30.5047073	5046	2.52	149.3	-1.24	0.46	Sgr
69373	283.7333679	-30.4932117	4977	2.37	144.5	-1.56	-0.21	M54
75429	283.7950134	-30.4848213	5028	2.50	149.3	-1.58	-0.19	M54
86412	283.7847900	-30.4922523	5079	2.56	146.1	-1.95	0.58	M54
91967	283.7814636	-30.4800529	4975	2.42	142.1	-1.86	0.47	M54
121249	283.7685242	-30.4917202	4873	2.32	153.5	-1.86	-0.07	M54
141357	283.7619019	-30.4915009	5023	2.51	146.1	-1.87	0.25	M54
155785	283.7575684	-30.4852924	5023	2.43	141.1	-1.66	0.26	M54
201571	283.7276917	-30.4915905	5015	2.46	144.4	-0.96	0.04	Sgr
208256	283.7915344	-30.4739513	5082	2.54	143.7	-1.93	0.16	M54
216867	283.7841797	-30.4684467	5007	2.47	142.7	-1.79	0.23	M54
231677	283.7753906	-30.4778271	5048	2.55	136.0	-1.70	-0.22	M54
235280	283.7738342	-30.4735279	5056	2.54	147.3	-1.66	0.53	M54
279832	283.7575073	-30.4666042	5090	2.56	148.6	-1.79	0.58	M54
299467	283.7481689	-30.4728985	4960	2.36	149.6	-1.72	0.27	M54
304691	283.7450256	-30.4665394	5005	2.48	139.0	-1.31	0.18	M54
315861	283.7359009	-30.4745407	5025	2.50	140.6	-1.60	-0.07	M54
335718	283.7800903	-30.4574833	5005	2.52	150.1	-1.67	-0.28	M54
340297	283.7754211	-30.4570541	4980	2.47	136.6	-1.63	-0.14	M54
342644	283.7732849	-30.4543114	5018	2.42	142.6	-1.62	0.10	M54
348795	283.7681274	-30.4567890	5002	2.41	149.6	-1.73	0.30	M54
356601	283.7614441	-30.4637871	5025	2.46	145.1	-1.59	0.53	M54
358028	283.7607117	-30.4514027	4928	2.36	144.2	-1.66	0.01	M54
359389	283.7593689	-30.4573898	5051	2.48	147.2	-1.37	-0.14	M54
379953	283.7375183	-30.4624958	5048	2.49	137.9	-0.90	-0.14	Sgr
1031659	283.7920227	-30.4277306	5002	2.38	161.6	-1.15	-0.07	Sgr
1031785	283.7452393	-30.5135555	5030	2.40	136.6	-1.12	0.03	Sgr
1032003	283.8471985	-30.3341923	5012	2.39	140.1	-0.71	0.21	Sgr
1032576	283.7683716	-30.4011650	4995	2.39	177.8	-1.25	-0.29	Sgr
1032677	283.6716309	-30.3297195	5033	2.41	151.0	-0.86	-0.15	Sgr
1033129	283.5857239	-30.4534187	4878	2.34	150.6	-0.79	—	Sgr
1033207	283.7309570	-30.5093040	5077	2.43	137.6	-0.90	-0.50	Sgr
1033253	283.7126770	-30.3716583	4864	2.33	145.8	-0.88	-0.71	Sgr
1033431	283.7608337	-30.6025276	4897	2.35	165.9	-1.14	-0.05	Sgr
1033794	283.8335571	-30.6086063	4953	2.38	142.7	—	—	Sgr
1033808	283.6697998	-30.5691261	4975	2.39	144.7	-0.91	0.03	Sgr
1034001	283.7369385	-30.4347324	4914	2.37	146.6	-1.68	-0.48	M54
1034068	283.7054138	-30.4942036	4982	2.40	141.2	-1.67	0.54	M54
1034166	283.6147766	-30.5109158	5074	2.44	102.8	-0.95	0.44	Sgr
1034215	283.6256104	-30.4640865	4883	2.35	162.6	-0.56	-0.49	Sgr
1034363	283.7250061	-30.4443989	4980	2.40	146.5	-1.48	0.24	M54
1034592	283.8386841	-30.4815445	4878	2.36	159.7	-0.47	-0.68	Sgr
1034628	283.8795471	-30.3539162	4990	2.41	144.3	-1.00	-0.62	Sgr
1034807	283.7220154	-30.3370037	4627	2.32	147.1	-0.46	-0.49	Sgr
1034871	283.6983032	-30.4932556	5002	2.42	148.2	-1.74	0.77	M54
1035051	283.5896912	-30.4579124	4975	2.41	149.7	-0.94	-0.98	Sgr
1035061	283.8948059	-30.4827633	4678	2.36	155.8	-0.83	-0.55	Sgr
1035450	283.7792969	-30.5218792	5074	2.46	142.8	-0.94	0.33	Sgr
1035614	283.6965637	-30.4720631	4706	2.38	141.5	-0.55	-0.71	Sgr
1035639	283.9363708	-30.3593540	4777	2.42	138.1	-0.55	—	Sgr
1035659	283.8937683	-30.5231647	5015	2.44	143.6	-1.77	-0.15	M54
1035689	283.6646118	-30.4083195	4892	2.38	125.6	-1.75	0.24	M54

Table 1 – *continued* Identification numbers, coordinates, effective temperature, surface gravity, radial velocity, [Fe/H] and [Na/Fe] abundances. Final flag indicates the membership to M54 or to Sgr.

ID	RA (J2000)	Dec (J2000)	T_{eff} (K)	log g	RV (km/s)	[Fe/H] (dex)	[Na/Fe] (dex)	flag
1035733	283.6871338	-30.5677834	5074	2.46	140.8	-0.90	0.23	Sgr
1035834	283.7239990	-30.4563236	4985	2.43	141.3	-1.55	-0.27	M54
1035938	283.7536316	-30.4476051	4997	2.43	123.1	-1.74	-0.32	M54
1035965	283.6389771	-30.5077534	4670	2.36	147.7	-0.39	—	Sgr
1036018	283.7001953	-30.5760975	4738	2.40	140.0	0.07	-0.40	Sgr
1036558	283.7184753	-30.4782505	4933	2.41	138.1	-1.66	-0.03	M54
1036741	283.7993469	-30.4916420	5015	2.45	137.5	-1.66	0.06	M54
1036890	283.8543091	-30.5144444	4716	2.40	116.0	-1.04	-0.24	Sgr
1037256	283.9817505	-30.4822559	4660	2.38	146.0	-0.56	-0.43	Sgr
1037298	283.7445984	-30.5185242	4911	2.41	158.1	-0.96	0.15	Sgr
1037347	283.5868835	-30.5343914	4747	2.43	151.9	0.24	0.15	Sgr
1037357	283.7287598	-30.3941364	4938	2.42	144.0	-1.55	0.27	M54
1037383	283.7582397	-30.4474907	5007	2.46	151.0	-1.58	0.38	M54
1037405	283.8029785	-30.6097832	4972	2.44	145.7	-1.40	—	M54
1037499	283.9023132	-30.5804310	5082	2.49	132.9	-1.15	—	Sgr
1037755	283.8068848	-30.4766140	5023	2.47	143.1	-1.50	0.27	M54
1037842	283.6522827	-30.4114075	4773	2.45	149.4	-0.84	-0.16	Sgr
1037956	283.7883301	-30.5176754	5087	2.50	129.4	-1.62	0.51	M54
1038371	283.7473450	-30.4219704	4687	2.41	130.4	-0.82	-0.78	Sgr
1038827	283.7271729	-30.4614105	5018	2.48	145.7	-1.64	0.07	M54
1038900	283.9519348	-30.5770645	4682	2.41	143.3	-0.30	-0.47	Sgr
1039247	283.7293701	-30.5351334	4972	2.46	146.1	-1.52	0.34	M54
1039380	283.6416626	-30.4188614	4764	2.46	123.5	-0.65	-0.26	Sgr
1039482	283.9963989	-30.4818535	4782	2.47	138.4	-0.64	—	Sgr
1039645	283.7586670	-30.5772209	4800	2.48	133.7	-0.27	-0.47	Sgr
1040277	283.8876648	-30.4286728	4807	2.49	142.9	-0.61	-0.49	Sgr
1040695	283.8935852	-30.6129131	4775	2.48	159.6	-0.10	—	Sgr
1040996	283.7201233	-30.5874443	4716	2.45	143.2	-0.47	-0.87	Sgr
1041212	283.7241211	-30.5361309	5043	2.52	144.3	-1.03	-0.09	Sgr
1041214	284.0014343	-30.5138874	4816	2.51	142.7	-0.06	—	Sgr
1041231	283.7814636	-30.6557369	4682	2.44	140.2	—	—	Sgr
1041308	283.8000793	-30.4399662	5046	2.52	149.8	-1.75	0.06	M54
1041392	283.7596741	-30.6370296	4798	2.50	160.3	0.52	-0.78	Sgr
1041896	283.8808899	-30.4472752	4718	2.47	133.9	-0.66	-0.52	Sgr
1041905	283.8525391	-30.4917564	4784	2.50	146.9	-0.61	-0.56	Sgr
1042086	283.8047180	-30.4664555	5020	2.52	142.2	-1.99	0.59	M54
1042102	283.7253723	-30.4827061	5085	2.55	143.9	-0.92	—	Sgr
1042123	283.7680359	-30.4397469	4916	2.47	141.1	-1.77	-0.11	M54
1042352	283.6452942	-30.4793129	4904	2.47	165.3	-1.25	-0.03	Sgr
1042739	283.7419739	-30.4234066	4950	2.49	146.3	-1.47	-0.22	M54
1043020	283.7697144	-30.5278034	4987	2.52	141.2	-1.87	—	M54
1043447	283.7137451	-30.3280296	4995	2.52	154.8	-1.51	-0.21	M54